

LONG CABLE APPLICATIONS WITH PM MOTORS AND MV DRIVES

Copyright Material IEEE
Paper No. PCIC-

Mukul Rastogi
Member, IEEE
Siemens Industry, Inc.
500 Hunt Valley Drive
New Kensington, PA 15068
USA
mukul.rastogi@siemens.com

David J. Liney
Shell
150 North Dairy Ashford
Houston, TX, 77079
USA
David.J.Liney@shell.com

Richard Broderick
Shell
3333 Highway 6
Houston, TX, 77082
USA
Richard.Broderick@shell.com

Richard H. Osman
Senior Member, IEEE
Siemens Industry, Inc.
500 Hunt Valley Drive
New Kensington, PA 15068
USA
dick.osman@siemens.com

Abstract—Subsea Pump applications commonly use induction motors due to their rugged design and simple construction. However, such motors operate at low power factor and efficiency. These issues are minimized with Permanent Magnet Motors (PMMs) that operate at higher power factor and lower currents. Lower stator current is desirable because losses are an important factor with long umbilical cables between drive and motor. A PMM also allows an increased rotor gap reducing hydrodynamic drag on the motor and enabling higher shaft speeds. In this paper, operation of a mud line pump (MLP) coupled to a medium voltage PMM that is powered by a medium voltage (MV) drive over a 10.5 km cable length is presented. Motor starting and operation under load disturbances are investigated to show drive and motor performance. Waveforms showing steady state operation are presented to show benefits of the MV drive. The overall benefits of a PMM as compared with an induction motor based on operating experience are included.

Index Terms — PM Motors, Medium Voltage Variable Frequency Drives, Long Cables, Motor Starting

I. INTRODUCTION

Development of technology has allowed oil and gas producers to place more equipment on the sea floor to process the fluid that is pumped up from within the seabed. This allows efficient use of platform space while reducing the amount of material handling and processing required above water. Underwater processing now includes Boosting, Separation, Treatment and Injection applications.

Subsea applications impose several unique requirements due to the flow of process fluid through the motor and distance between the driven equipment and the variable frequency drive (VFD). In such applications, the umbilical (or cable) between the drive and motor is the most expensive component. Hence, operating at the lowest possible current rating at any given load becomes important. This reduces the copper required in the cable and decreases its cost, weight and operating losses. The presence and flow of fluid through the motor airgap creates a drag on the rotor, which requires as large of a gap as possible to reduce hydrodynamic drag. In some cases, the fluid can be at a high temperature making it important for the rotor losses to be minimized to allow operation at acceptable temperatures.

Induction motors (IM) have traditionally been the motor of choice for subsea applications due to their rugged design and

simple construction. However, the subsea requirement of a large air-gap increases the no-load current of the motor and reduces the operating power factor, which in turn increases the operating current as well as the required cable current rating. Rotors of induction motors, although simple to build, have operating losses that need to be managed through machine design so that the available cooling in the application does not result in excessive temperatures. In comparison, permanent magnet motors (PMM) with magnets on the rotors operate with minimal no-load current and significantly lower rotor losses. According to one manufacturer of IMs and PMMs for electric submersible pump applications, the typical operating power factor (PF) PMMs is 0.96 as compared with 0.86 PF for IMs [1]. The use of magnets results in a reduction of the rotor back-iron allowing smaller rotor diameter and larger air-gap [2]. These advantages make them ideal for subsea applications. High speed operation is also possible with PMMs as a result of the reduced drag. However, PMMs cannot be operated at high temperatures where demagnetization can occur. Also, a rotating machine would always back-feed the drive even when it is shut-down, which would require additional monitoring and/or safeguards.

Operation of the drive output at medium voltage (MV) allows further reduction of cable costs because the savings due to the reduction in copper are more than the expense for additional insulation material. An improvement in system efficiency is also obtained. Reference [3] provides a detailed comparison of the two solutions in terms of different aspects of the drive system including output transformer, input harmonics and effects of input power quality. Medium voltage PMMs are offered by many manufacturers of subsea motors and pumps. This requires the drive to provide MV output, which can be realized with either a low voltage (LV) drive with a step-up output transformer or a MV drive. Both solutions are very popular.

The former solution is simple because of the use of a LV drive, but requires an input filter, an output transformer and possibly an output filter. The transformer rating, which is directly influenced by the cable resistance voltage drop and starting torque requirement for the application, can be significantly higher than the motor kVA for long cable lengths resulting in increased size, cost, and reduced system efficiency [4].

The latter – MV drive – solution can be realized using several available topologies in the market [5], all of which avoid the use of an output transformer but may include an output filter. The rating of the filter is 5-20% of motor kVA rating as compared with a fully rated or larger transformer at the output of a LV drive

[6]. The following section describes the differences and advantages of available MV drive solutions.

In this paper, a Mud Line Pump application consisting of a PMM, a long cable (also referred to as umbilical) and a MV drive is presented. The capability of the system to meet the application requirements is shown through simulation results and measured data from the actual application. The benefits of this system over other systems are described based on implementation and operating experience. Simulation results are presented in Section V and measured data from the actual application is shown in Section VI.

II. MV DRIVE SOLUTIONS

Medium voltage PMMs are now available from many manufacturers. But there are only a few MV VFD topologies commercially available. These are listed below:

1) *Current-source technologies*, where the line side converter maintains a constant DC link current and the DC link filter is an inductor [7]:

- Current-source with capacitors on the load – These drives are now used for very large, tens of MW rated applications, where bulk power is required and where the engineering cost of applying the drive to the end user's power system can be justified.
- Current-source load commutated (LCI)
- Current-source with self-commutating SGCT's

2) *Voltage-fed technologies*, which have a constant DC link voltage and the DC link filter is a capacitor:

- Voltage-fed neutral point clamped (NPC) [8].
- Voltage-fed multi-level.
 - Cascaded H-bridge (CHB) [9]
 - Modular multi-level (M2C or MMC) [10]
 - Flying capacitor based active NPC [11]

Among MV VFDs, the multi-level voltage fed topologies have several features that make them very suitable for subsea, long cable applications. These are:

- i. Improved output waveform quality, with the following characteristics:
 - Low output current distortion of less than 3%
 - Low output torque pulsations
 - Lower peak voltages when compared with other MV topologies
 - Lower output voltage rise time in the range of 1-3 kV/ μ s
 - Reduced cable charging current
 - Lower switching frequency of hundreds of hertz to obtain the improved output waveform quality described above; this results in reduced converter losses, typically less than 1%
 - Smaller output filter components
- ii. Extremely low input harmonic currents due to multi-pulse (18-pulse to 48-pulse) input circuit.

- iii. Constant high input power factor (> 0.95) due to the use of input diode rectifiers. The reactive power requirements of the load are not passed on to the input. In comparison, current-source topologies with thyristor front-ends have input power factor (PF) that follows the motor (or output) PF.
- iv. Fault-tolerant topology from multiple cells with bypass capability. Multi-level, modular topologies can continue to operate with any failed component within a module [12]. However, topologies with series-connected semiconductors can offer continued operation in the presence of failed semiconductor(s) but are not tolerant to failures in other components, such as gate drive circuit(s).
- v. Minimal common-mode voltage on motor due to input transformer.

III. LONG CABLES AND PMMs

The use of long cables also imposes requirements on the waveform quality of drive output. This is due to the standing wave effect that occurs when drives produce waveforms with voltage steps at one end of a conductor that are reflected by the mismatch between the conductor and motor impedances and the motor impedance at the other end. If the output step rise time is significantly less than the transit time through the cable, amplification of the step can occur at the motor. The result is an amplification of drive harmonics resulting in motor waveform distortion [13]. Cable properties, such as resistance, can influence the starting capability of the system if care is not taken when selecting the appropriate drive control method. In this application, the selection of the MV drive and the cable impedance were such that the drive output voltage would operate at its rated value with the motor at nearly 60% of maximum speed. Above this speed, the drive had to maintain constant motor voltage, i.e. operate in field weakening. The main concern was PMM control over the entire speed range including the field weakening region. There was also a concern that not having feedback of the rotor position would cause oscillations when starting and nuisance pole-slip conditions.

These concerns were mitigated using simulations, which were also used to determine the type of output filter that would suffice for the application.

IV. SYSTEM DESCRIPTION

A. Mud Line Pump Application

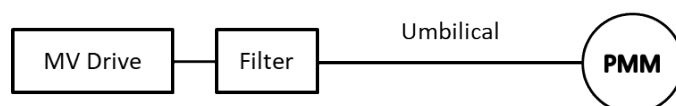


Fig. 1 One line diagram of the system

The mud line pump is situated in 1200 m of water off the coast of Brazil and is powered from a floating facility via a 12, 20(24)

kV, 95 mm² trefoil (one of three in the hybrid umbilical). Electrical connection on the seafloor is via wet mate connectors and a pressure housing penetrator to the stator windings. The mud line pump may be connected to a variety of subsea wells through a network of flowlines and manifolds.

B. Component Specifications

- Motor: PMM, 5245 V, 190 A, 1.24 MW, 53.3 Hz, 3200 rpm, 90 Hz max frequency
- Cable: 10.5 km, $R=0.270 \Omega/\text{km}$, $L=0.341 \text{ mH}/\text{km}$, $C=0.220 \mu\text{F}/\text{km}$
- Drive: CHB, 18-cells, 6.6 kV, 260 A output

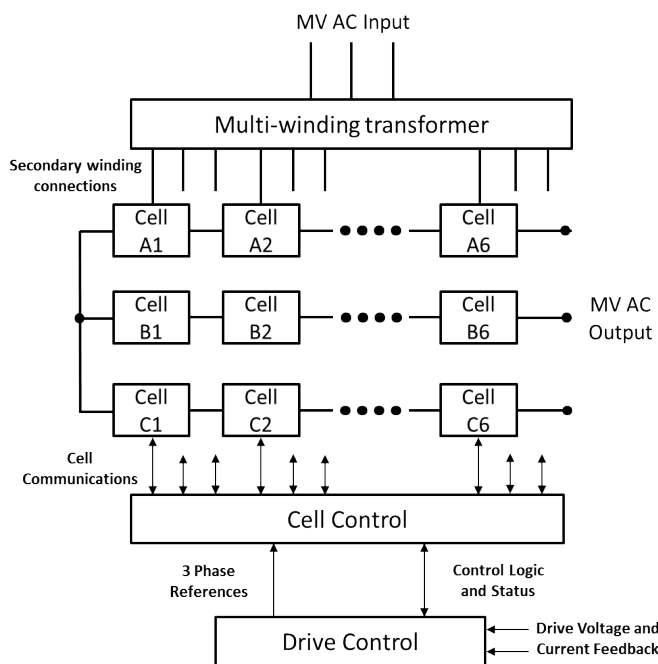


Fig. 2 (a) Drive block diagram

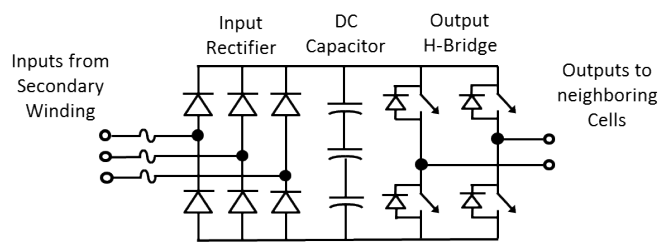


Fig. 2 (b) Simplified schematic of a power cell

C. MV Drive and Control

The MV drive used in this application is a Cascaded H-Bridge (CHB) inverter consisting of 6 inverters (referred to as "cells" in this paper) per-phase. Figure 2(b) shows the power components in each cell - a 3-phase input rectifier, dc-capacitor bank and a single-phase H-Bridge inverter at its output. The input rectifier is fed from a dedicated 3-phase secondary winding of a multi-

winding input transformer. The primary winding is fed from the 6.6 kV line on the platform. The outputs of the cells are connected in series to form one output phase of the drive.

Each cell communicates with the central cell controller to receive control commands and send status signals. The cell controller generates the switching commands for each cell based on the 3-phase voltage commands received from the drive controller. In response, each cell controller sends cell status and cell feedback to the drive controller.

Figure 3 shows the control block diagram used for this drive. The overall control operates almost the same as sensorless vector except that the motor is started using open loop i/f control (indicated with subscript OL) up to a pre-determined transition speed (ω_{TR}) [14, 15]. In this starting mode, the torque current ($i_{qsRef,OL}$) is ramped up to a level corresponding to the expected stiction torque for the application after which the speed reference is ramped up to the transition speed. After a short dwell period at the transition speed, during which the control begins to use outputs from the Motor & Cable Model, the drive resumes motor acceleration to the desired speed demand.

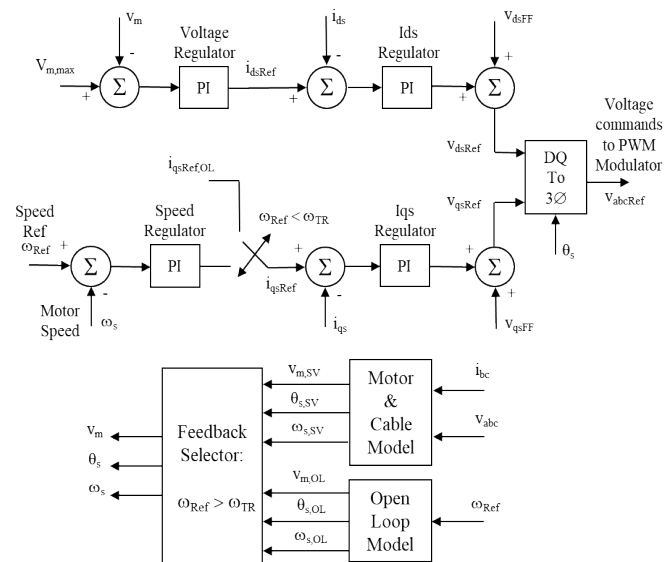


Fig. 3 Control block diagram

The Motor & Cable Model uses drive output currents (i_{bc}) to estimate rotor position by subtracting off the voltage drops in the output filter, cable impedance and motor inductance from the drive output voltages (v_{abc}). An estimate of motor voltage (v_m) is also provided by this function block.

The voltage regulator is effective only when the motor voltage exceeds its rated voltage (or its maximum operating voltage $V_{m,max}$). Above base speed, it provides a negative value of i_{dsRef} to hold motor voltage at the desired maximum value. Below base speed, the voltage regulator output (or i_{dsRef}) is limited to zero. This provides maximum torque-per-amp control for non-salient pole PM motors.

Feed-forward components v_{disFF} and v_{qsFF} compensate for the cross-coupling terms arising from the inductive and capacitive elements in the d-q reference frame. These can be used if high performance is desired.

V. SIMULATION RESULTS

For this application, simulations were used to verify starting torque capability, output filter design, steady state, and transient drive and motor operation. Key results are shown in this section.

The simulated system is shown in Fig. 4. The complete drive control is simulated along with a model of drive including power cells and PWM modulator, drive filter, long cable and PMM.

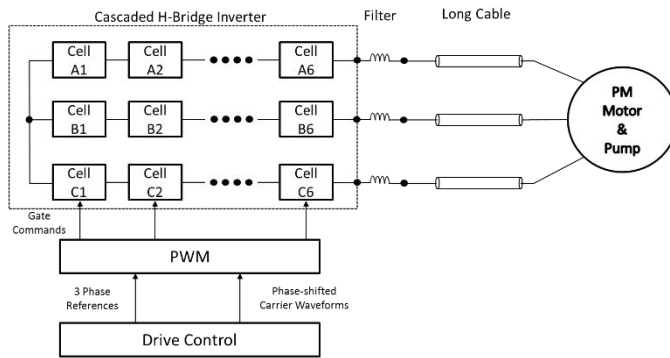


Fig. 4 Block diagram of the simulated system

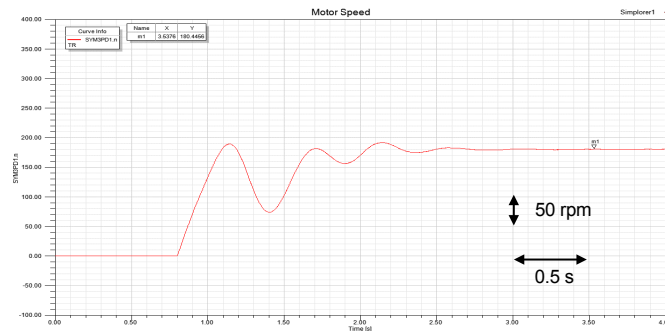


Fig. 5 Motor speed when starting in i/f mode

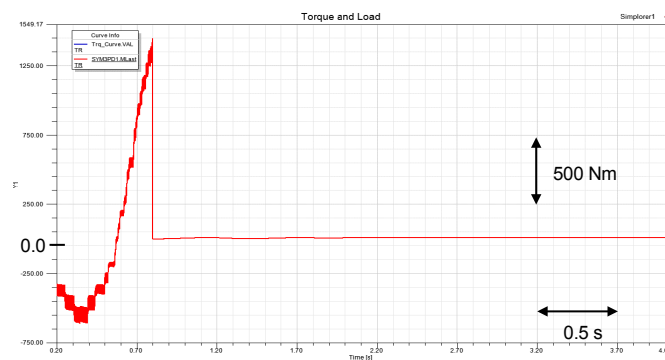


Fig. 6 Motor torque developed when starting in i/f mode

A. Motor Starting

The application required a starting torque of 1500 Nm, for which the starting current, frequency and ramp rates were determined through simulations. Figures 5 - 7 show the motor speed, torque and currents, respectively, with 150 A current at 3 Hz and a starting ramp of 2 sec. In Fig. 6, motor torque increases above

1500 Nm at time $t = 0.80$ s when the motor begins to move (refer Fig. 5). As soon as the shaft begins to rotate, the motor torque falls to the normal level based on a quadratic load torque characteristic. Motor speed shows some oscillations due to the low mechanical damping in the motor/pump mechanical system. Motor currents remain sinusoidal except when there is fast change in motor speed.

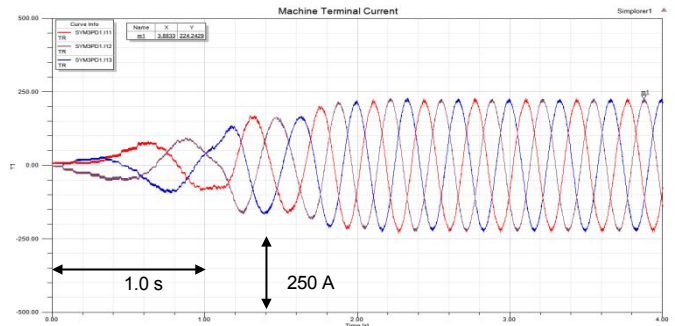


Fig. 7 Motor phase currents when starting in i/f mode

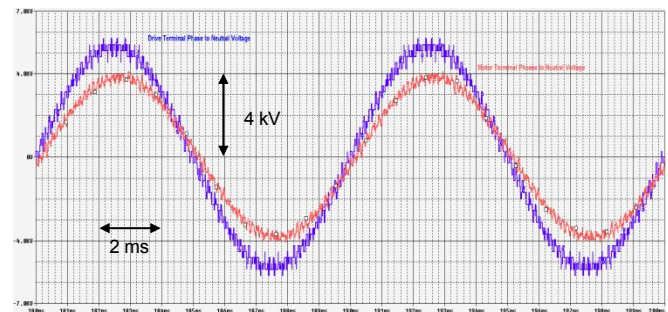


Fig. 8 Drive terminal (L-N) voltage (blue) and motor terminal (L-N) voltage (red) with reactor only filter

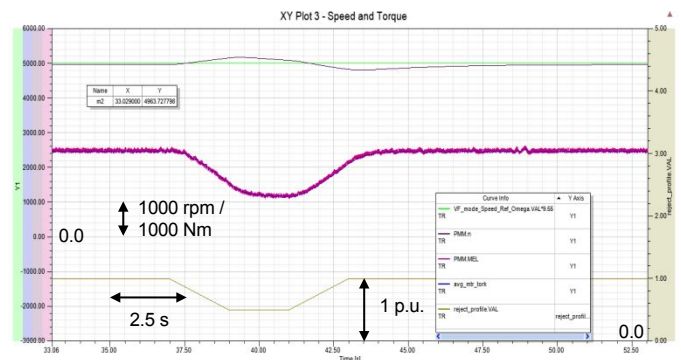


Fig. 9 Motor speed reference (green), motor speed (purple), motor torque (purple) and load torque profile (grey) during a load transient.

B. Steady State Operation with Output Filter

The requirement and design of an output filter was determined using simulations. Without a filter, the drive switching frequency components were found to be amplified by the resonance frequency of the output cable. Using simulations, a reactor only filter (with a value of 2.5 mH per-phase or 5.25% of motor base

impedance) that allowed the motor voltage distortion to be below the drive output voltage distortion was found. The motor terminal voltage and drive output voltage are shown in Fig. 8 with the reactor only filter.

C. Effect of Load Transient

A load transient was applied in order to simulate the effect of a gas-pocket on drive/motor operation. The load torque is adjusted to have a profile representing the flow of a gas-pocket through the pump and is shown in Fig. 9. The torque ramp times are each 2 s long with a 2 s dwell time at 50% torque. The effect on motor speed and torque are shown in this plot. The maximum motor speed deviation is 180 rpm, with the motor operating at 5000 rpm (or 83.3 Hz), while the drive maintains control of the motor.

VI. MEASURED DATA

In this section, data captured during the commissioning of the system is presented. Motor starting, steady state operation and the onset of field weakening (or Phase Advance) are shown in the following figures. The variables shown in the data plots are defined in Table I.

TABLE I
LIST OF VARIABLES SHOWN IN PLOTS

Name	Description	Scaling
Speed Ref	Speed Reference to Drive	1.00
Mts Speed	Motor Speed	1.00
Flux DS	Motor Flux	1.25
Ids ref	Motor d-axis current reference	1.00
Ids	Motor d-axis current	1.00
Iqs ref	Motor q-axis current reference	1.00
Iqs	Motor q-axis current	1.00
Drv State	Drive Status Flag (Run, Idle, Stop, etc.)	NA
Neutral Vlt	Drive Neutral Voltage	1.00



Fig. 10 Drive variables during motor start in i/f mode and transition to sensorless vector control

A. Start-up

Motor starting is shown in Fig. 10. An initial current ramp of 60% over a 2 s period is used. The frequency is ramped up to 10 Hz (or 18.7%) while operating in open loop mode (i/f control). The

drive transitions to sensorless vector control above this speed. This transition speed was selected because at that speed, motor back-emf would exceed the cable impedance drop, thus allowing the sensorless vector control algorithm to sense the rotor angle accurately. As the drive transitions from i/f control to sensorless vector control, the motor accelerates while the torque current reference decreases from the fixed starting current level to the level required to maintain motor operation.

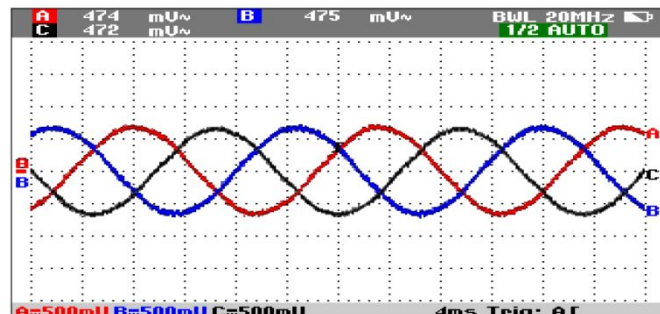


Fig. 11 (a) Drive currents under light load at 52Hz, 4.44kV, 65A



Fig. 11 (b) Drive variables under light load at 52Hz. Speed Reference and Motor Speed signals are offset by -0.80.

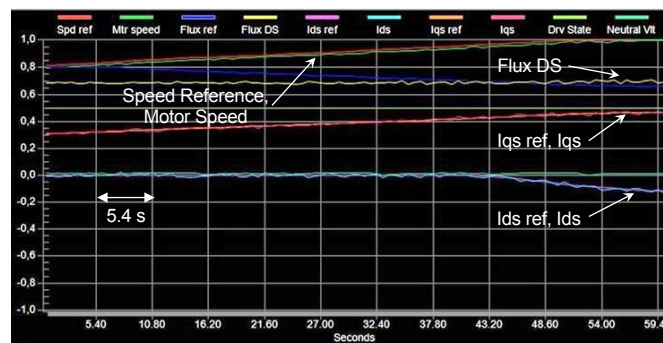


Fig. 12 Drive variables during onset of field weakening

B. Steady State and Acceleration

Operation of the motor at near rated speed (52 Hz) and light load (34%) is presented here. Figure 11(a) shows the drive output currents that are nearly sinusoidal, and Fig. 11(b) shows the drive variables.

Motor acceleration through rated speed is shown in Fig. 12. Above rated speed, the drive begins to limit the motor terminal

voltage by changing motor power factor. This is observed as a change in the magnetizing component of current, I_{ds} , which is normally at zero.

C. Benefits of Selected Components

A comparable induction motor (IM) in an ESP (Electric Submersible Pump) application would have approximately 15% lower power factor and 10% lower efficiency than a PMM. This would mean that an IM with the same voltage and current rating as the PMM would have a rating of 980 kW. In other words, the system with a PMM can provide 26.5% more torque and power. Moreover, the PMM can operate up to 90 Hz, while a typical IM can be operated up to 67 Hz.

The PMM design is smaller in size than a comparable IM by 30-40% in weight making installation easier and less expensive in terms of infrastructure required to put it into place. As mentioned in the Introduction, PMMs can have a larger airgap resulting in reduced hydrodynamic drag on the fluid flowing through the motor, and higher process efficiency.

When comparing MV and LV drive solutions, the efficiency is in favor of the former due to the lack of (a) input filtering and (b) an output transformer. A LV drive with a 2-level output would require a substantially larger output filter to limit the distortion at the motor terminals. With these considerations, the improvement in efficiency with a MV drive is greater than 2%. This small improvement in efficiency is important when a MV drive with 97% efficiency is available and can provide significant savings (40%) in the cooling capability needed if drive installation is in a controlled environment.

VII. SUMMARY

Developments in subsea processing have led to an increasing number of applications that can be located on the seabed. This, in turn, has increased the distance between the drive equipment and the electrical drive necessitating the use of long cables. In such systems, the subsea cables form a substantial portion of the overall investment costs. The selection of the appropriate transmission voltage and, the type of motor and drive topology each have an important effect on costs of the cable. This paper presents a subsea mud line pump application that is driven by a PMM connected to a MV multi-level drive with a 10.5 km long cable. The advantages of each of these system components over available options are described. Verification of drive operation is presented using simulation results. Data from drive commissioning is presented to demonstrate successful operation in the field.

VIII. REFERENCES

- [1] Borets, *Artificial Lift Technologies Catalog*, 2015, pp 168-179.
- [2] D. Zechmair and K. Steidl, "Why the Induction Motor could be the better choice for your Electric Vehicle Program," in *World Electric Vehicle Journal*, vol 5, 2012, pp 546-549.
- [3] White Paper: Cost Considerations When Selecting Variable Frequency Drive Solution. Online at

<https://new.siemens.com/us/en/products/drives/sinamics-electric-drives/perfect-harmony.html>.

- [4] R.O. Raad, T. Henriksen, H.B. Raphael and A.H-Jacobson, "Converter-fed Subsea Motor Drives," *IEEE Transactions on Industry Applications*, vol 32, no 5, Sep./Oct. 1996, pp 1069-1079.
- [5] M. Hiller, R. Sommer and M. Beuermann, "Medium-voltage Drives," *IEEE Industry Applications Magazine*, Mar./Apr. 2010, pp 22-30.
- [6] M. Smoczek, T.F. Pollice, M. Rastogi and M. Harshman, "Long Cable Application from a Medium-Voltage Drives perspective," *IEEE Transactions on Industry Applications*, vol 52, no 1, Jan./Feb. 2016, pp 645-652.
- [7] B. Wu and M. Narimani, *High-power Converters and AC Drives*, Second Edition, Hoboken, NJ: John Wiley & Sons, Inc. 2017.
- [8] P.K Steimer, J.K. Steinke and H.E. Gruning, "A reliable, interface-friendly Medium Voltage Drive based on robust IGCT and DTC Technologies," in *IEEE-IAS Annual Meeting Conference Record*, 1999, pp 1505-1512.
- [9] P. W. Hammond, "A New Approach to enhance Power Quality for Medium Voltage Drives," *IEEE Transactions on Industry Applications*, vol 33, no 1, Jan./Feb. 1997.
- [10] M. Glinka, and R. Marquardt, "A New AC/AC Multilevel Converter Family," *IEEE Transactions on Industrial Electronics*, vol 52, no 3, pp 662-669, June 2005.
- [11] P. Barbosa, P. K. Steimer and M. Winkelkemper, J. Steinke, and N. Celanovic, "Active-neutral-point Clamped (ANPC) Multilevel Converter Technology," in *Proceedings of EPE Conference*, 2005, pp 11-14.
- [12] P.W. Hammond, "Enhancing the Reliability of Modular Medium-Voltage Drives," *IEEE Transactions on Industrial Electronics*, vol 49, no 5, Oct. 2002, pp 948-954.
- [13] A.F. Moreira, T.A. Lipo, G. Venkataramanan and S. Bernet, "High-Frequency Modeling for Cable and Induction Motor Overvoltage Studies in Long Cable Drives," *IEEE Transactions on Industry Applications*, vol 38, no 5, Sep./Oct. 2002, pp 1297-1306.
- [14] L. Xu and C. Wang, "Implementation and experimental investigation of Sensorless Control Schemes for PMSM in Super-high Variable Speed Operation," in *IEEE-IAS Annual Meeting Conference Record*, 1998, pp 483-489.
- [15] A. McIntyre, J. Andrews, G. Davis, P.W. Hammond and M. Rastogi, "Medium Voltage Drives for Sub-sea Applications – Evaluation with 23.5km Cable Length," *ESP Workshop*, 2002.

IX. VITAE

Mukul Rastogi received the B.Tech. degree from the Indian Institute of Technology, Madras, in 1991 and the M.S. and Ph.D. degrees from the University of Minnesota, Minneapolis, in 1993 and 1996, respectively. Since 1996, he has been with Large Drives, Siemens (formerly Robicon Corporation) and has worked on the development and application of ac motor drives and power supplies. He is currently the manager of the Power Electronics Development group. He has co-authored 10 technical papers and holds over 20 patents.

David J. Liney received his MA Hons in engineering from Cambridge University in 1994 and Ph.D. in high temperature superconductivity in 1997. He has worked within the oil and gas industry for over 20 years, specializing in subsea power systems and fibre optic sensing.

Richard Broderick received his B.S. in electrical engineering from the University of Texas at Austin in 2008. He has worked in the oil and gas industry for 12 years, specializing in the field deployment of novel technologies for subsea applications.

Richard H. Osman received the BSEE degree from the Carnegie Institute of Technology, Pittsburgh, PA, in 1965. He

worked for Westinghouse Electric Corporation at the Research and Development Center from 1965-1970. He was responsible for the development of a variety of solid-state variable speed drives such as, thyristor DC drives, cyclo-converters, and inverters. He joined the Robicon Corporation in 1970 as a Drives Development Engineer. Since the acquisition of Robicon by Siemens, he is a Principal Engineer at Siemens Industry, Inc. He served as the technical advisor to the Company and worked closely with the product development group at Siemens.

Mr. Osman is a Senior Member of the IEEE. He has written several technical papers on variable frequency drives and is a Registered Professional Engineer. He is an expert user of Ansys Maxwell and Simplorer.